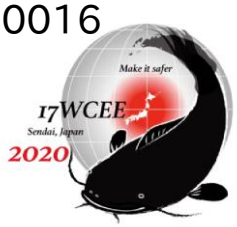

Estimation of Q values in the Sedimentary Layer of the Kanto Basin Using Envelopes of Later Phases

H. Yoshida[(1)], Y. Sato[(2)]

[(1)] *Associate Chief Researcher, Research & Development Institute, Takenaka Corporation, yoshida.haruo@takenaka.co.jp*
[(2)] *Group Leader, Research & Development Institute, Takenaka Corporation, satou.yoshiyukia@takenaka.co.jp*

Abstract

Long-lasting and long-period ground motions in large-scale basins that are excited due to large earthquakes are essential to evaluate when planning the structural design of high-rise or base-isolated buildings. In order to ascertain the duration and amplitude of these seismic waves by numerical analysis, the damping characteristics of subsurface structures (Q-value of sedimentary layers) must be evaluated appropriately. In this paper, we estimate the Q-values of the Kanto basin from the attenuation model of surface waves using later phases of records observed in the metropolitan area seismic observation network ("MeSO-net").

The first step of our analytical procedure entailed the application of band-pass filters centered on target periods to the two horizontal components of the velocity waveform recorded at the ground surface. Multiple envelopes of the square amplitude were also calculated. Next, Q values corresponding to each target period were calculated by minimizing the sum of the squares of errors between the envelope and the surface wave distance attenuation model. Finally, Q-values were estimated from the Q-value regression model of each period.

In order to verify the usefulness of this method, we applied it for numerical simulation results, which were calculated using different underground structure models. Observation points were set at five sites in the Kanto basin, and the epicenter was set as a point source (Mj4.3, depth 27km). The velocity structure model published by the Headquarters for Earthquake Research Promotion was used as the underground structure model. The Q value of the simulation was set by $Q = Q_0 f / fr$ (Q_0: Q value at reference frequency, fr: reference frequency), and this value is proportional to the frequency. We established four cases with different Q value conditions, where the Q_0 of the sedimentary layer was set at 150, 200, 250, Vs / 5 (cases 1 to 4). Vs means shear wave velocity. In all cases, the fr was set at 0.5 Hz.

The estimated Q values in cases one to three exhibited little variation at frequencies of 0.2 Hz or higher. We were able to confirm that the Q value of the sedimentary layers in the simulation was well estimated based on the average attenuation of the envelope of the surface wave parts of ground motions. We found that the variation in the estimated Q value at each observation point was small from the estimated Q value in Case 4 (Q values set as Vs / 5). This led us to expect that the influence of the difference in the underground structures at each point is small. We also confirmed that the average Q value of the entire basin could be estimated by our proposed method.

We estimated the Q values of the Kanto basin using observation records of 6 earthquakes of Mj6 or higher. The central period for the Q value estimation was set in 1-second increments between 2 and 10 seconds.

We also observed Q values of 160 to 380 at 0.1 to 0.5 Hz. The regression equation was calculated as $Q = 490f^{0.41}$ for the frequency of 0.125 Hz or higher (period of 8 seconds or less), where the slope of the Q value is stable.

Keywords: Q value, sedimentary layer, Kanto basin, long-period earthquake ground motion, MeSO-net

1. Introduction

In order to accurately evaluate the duration and amplitude of waves following long-period ground motions associated with major earthquakes in large-scale basins, the appropriate damping characteristics (Q value) must be utilized as a part of numerical analysis. Kagawa [1] estimated the Q value for the period of 2 to 8 seconds in the Osaka Plain from the attenuation characteristics of the envelopment waveform following the observation record. Yoshida et al. [2] estimated the Q value of the Kanto basin with the assumption of body waves using the method of Kagawa [1]. In this paper, the Q values of the Kanto basin are estimated from regression equations based on the attenuation characteristics of surface waves using later phases of records observed by the Tokyo Metropolitan Area Earthquake Observation Network (MeSO-net) [3].

2. Overview of the estimation method

Our analysis was performed according to the procedure of Yoshida et al. [2]. First, the envelope of the square amplitude was calculated using the method of Dziewonski et al. [4] after applying a band-pass filter centered on the target period to the two horizontal components of the ground surface velocity waveforms. These two components were composited using the square root of the sum of squares. Next, a Q value minimizing the sum of the squares of the error between the square envelope form and Eq. (1) was calculated. Here, t indicates the elapsed time from the time of occurrence, and the geometric attenuation of the surface wave is represented by 1/t because the square amplitude is used.

$$y = \frac{1}{t} exp\left(\frac{-2\pi \cdot f \cdot t}{Q(f)}\right) \tag{1}$$

The central period for estimating the Q value was set at intervals of 1 second between the 2 to 10 second periods. Figure 1 presents an example of an analysis using observation waveforms at points on the Kanto basin.

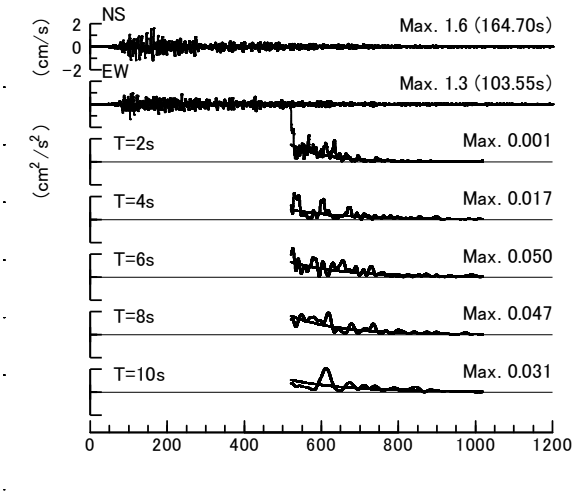

Fig. 1 – Example of observed and analyzed waveforms (MNAM site, 2014/11/22 northern Nagano earthquake)

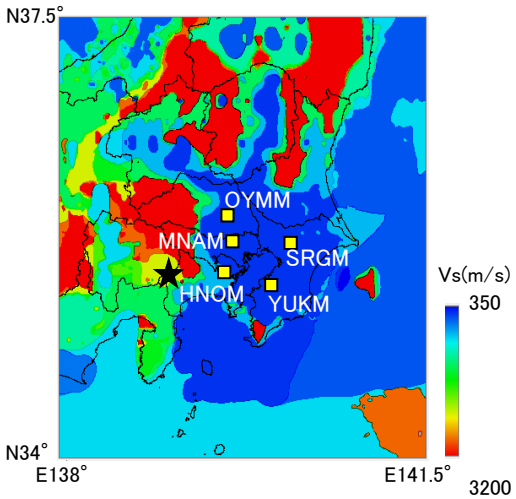

Fig. 2 – The epicenter of the earthquake used in the simulation (★), observation point (□) and underground structure model (GL-200m section)

3. Q value estimation by simulation

In order to confirm the applicability of our method for Q value estimation, an analysis using the calculation wave by the difference method was performed. Figure 2 shows the MeSO-net observation points used for our study, along with the epicenter of the earthquake used for the verification of our method. The observation points were five points on the Kanto basin, and the epicenter was a point epicenter (Mj4.3, 27 km deep). The nationwide primary model [5] in the range shown in Fig. 2 was used as the underground structure model. Since the thickness of the Kanto basin is less than 10 km, the grid spacing was 200 m for GL-10 km or less and 600 m for GL-10 km or less. It was also 50 km in depth. The Q value of the simulation is represented as $Q = Q_0 f / fr$ (Q_0: Q value at the reference frequency, fr: reference frequency) proportional to the frequency. The Q_0 of the sedimentary layer was set to 150, 200, 250, and Vs / 5 in cases one to four, respectively, while fr was set to 0.5 Hz. Table 1 shows an underground structural model just below central Tokyo. For the source time function, a smoothed ramp function with a rise time of 0.05 s was used. The program of the difference method used GMS [6]. GMS is a three-dimensional difference method strong motion calculation tool created by NIED.

Table 1 – Underground structure model under central Tokyo

No.	Vs (m/s)	Vp (m/s)	ρ (t/m3)	Q			
				Case 1	Case 2	Case 3	Case 4 (Vs/5)
1	500	1800	1.95	150	200	250	100
2	900	2300	2.1				180
3	1500	3000	2.25				300
4	3200	5500	2.65	640	640	640	640

Figure 3 illustrates a comparison example (Q_0 = 250) between the envelopes and the approximate curves. The envelope waveforms with a period of 2 to 10 seconds were estimated, and we confirmed that a seismic waveform duration equal to approximately 400 seconds could be accurately estimated up to a period of 10 seconds. When the period was 6 seconds or less, the estimation could be accurately performed even if the duration of the earthquake waveform was about 200 seconds.

Figure 4 shows a comparison between the estimated Q value and the set Q value in cases one to three. The red circle indicates the average value of five points for the estimated value, and the red horizontal line represents the standard deviation. The variation of the estimated Q value was small (above 0.2Hz), and the average value of all observation points was nearly the same as the set Q value. Therefore, we confirmed that the Q value given as the attenuation characteristic of the medium in the simulation could be estimated by the average attenuation of the envelope shape.

Figure 5 presents the estimated Q value of each observation point at 0.1 to 0.2 Hz in case three, where the variation was largest. The values other than OYMM were observed to nearly match the set Q value. Since OYMM is located at the outer edge of the basin, surface wave interference may have affected the estimation accuracy. The Q values of the other four points exhibit little difference, however, indicating that it may be possible to estimate the average Q value regardless of the location. The exception to this is an observation point, such as OYMM. We believe that the stability of the Q value in this method needs to be studied in the future. For example, the Q value stability can be ascertained by increasing the number of observation points in the central and surrounding areas of the basin. Figure 6 shows the estimated Q value for Case 4. Table 2 displays the set Q value [Vs / 5] that correspond to the average Vs of the sedimentary layer immediately below each point. This helps confirm that the estimated Q value variation at each observation point was small. The influence of the difference in the underground structure at each point was relatively small, making it possible to estimate the average Q value of the entire basin.

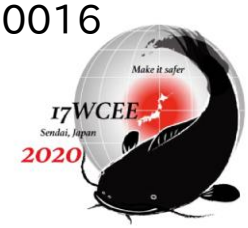

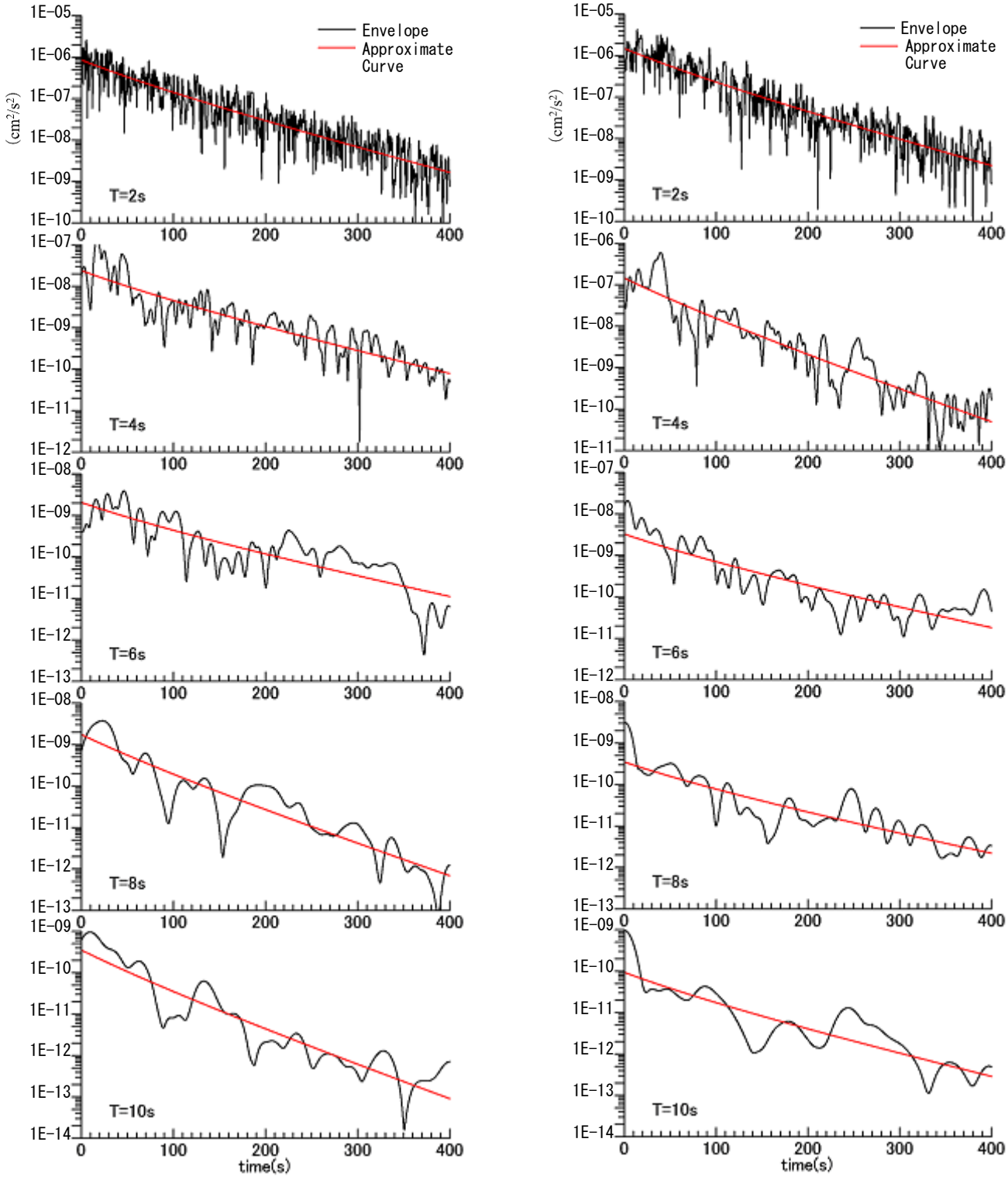

(a) YUKM (b) OYMM

Fig. 3 – Comparison of envelope and approximate curves in the Q_0 = 250 model

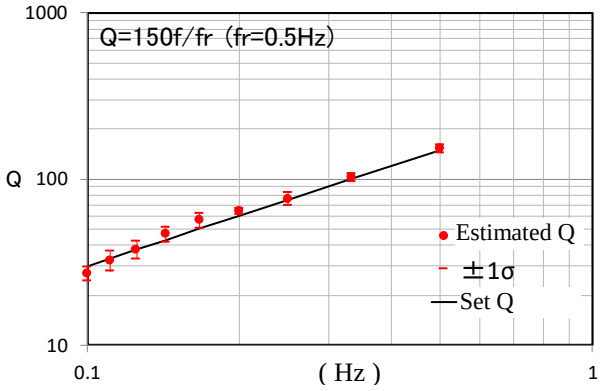

Case one

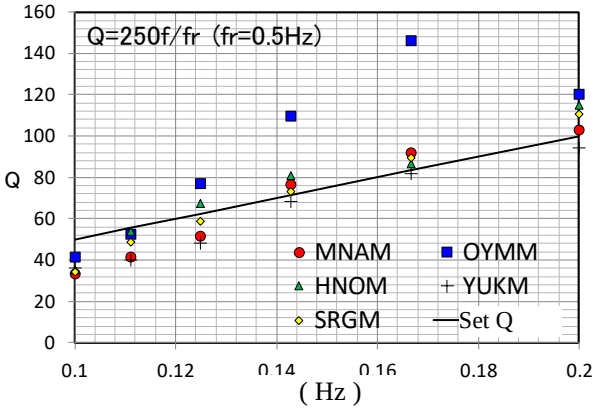

Fig. 5 – Comparison of the estimated Q value for each location (0.1-0.2Hz, Q_0 = 250 model)

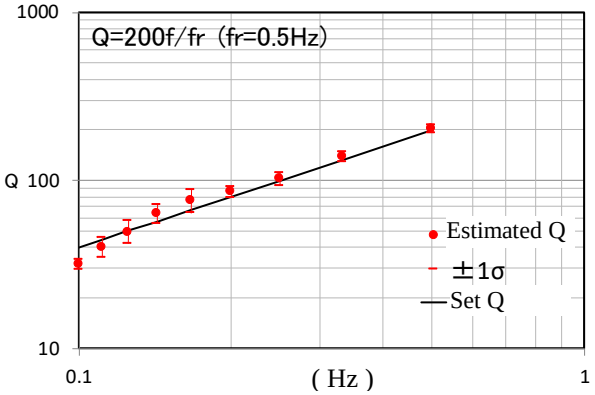

Case two

Table 2 – Average Vs and Q_0 (Vs / 5) below the observation point

Observation point	MNAM	HNOM	YUKM	SRGM	OYMM
Average Vs(m/s)	1112	1289	1148	1043	1246
Q_0(Vs/5)	222	258	230	209	249

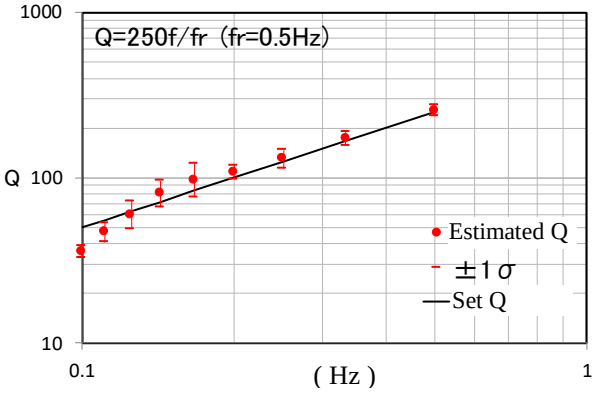

Case three

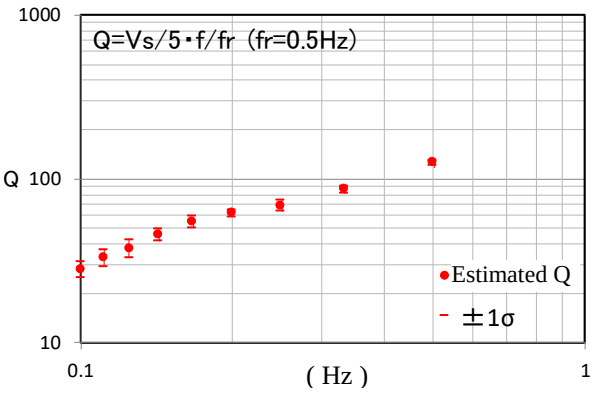

Case four

Fig. 4 – Comparison of estimated Q value and set Q value in Q_0 = 150 (Case one) ・200 (Case two) ・ 250 (Case three) models

Fig. 6 – Comparison of estimated Q value and set Q value in Q_0 = Vs / 5 (Case four) model

4. Q value estimation from observation records

The Q values were estimated using the observation records of the earthquakes shown in Table 3 for six earthquakes equal to or exceeding Mj6. Figure 7 illustrates the epicenter distribution of the observed earthquakes and the locations of the observation points. Figure 8 gives an example of the observed waveforms. The duration of seismic motion was confirmed to exceed 1000 seconds. The time range (500 s) in which the Q value was estimated is indicated by a solid line. Figure 9 gives an example of a comparison between the envelopes and the approximate curves (No. 6 earthquake). In a similar manner to the simulation method, we confirmed that the envelope waveforms could be roughly approximated for a period of 2 to 10 seconds.

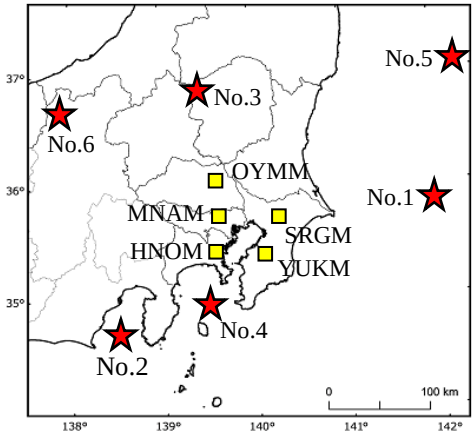

Fig. 7 – Epicenter (★) and MeSO-net observation point (■) used to estimate the Q value from observation records

Table 3 – Earthquake specifications *

No.	Origine date and time	Depth (km)	Mj	Epicenter
1	2011/03/13 10:26	11.18	6.6	FAR E OFF IBARAKI PREF
2	2011/08/01 23:58	23.03	6.2	SOUTHERN SURUGA BAY REG
3	2013/02/25 16:23	2.84	6.3	NORTHERN TOCHIGI PREF
4	2014/05/05 05:18	156.08	6.0	SAGAMINADA
5	2014/07/12 04:22	33	7.0	E OFF FUKUSHIMA PREF
6	2014/11/22 22:08	4.59	6.7	NORTHERN NAGANO PREF

*JMA

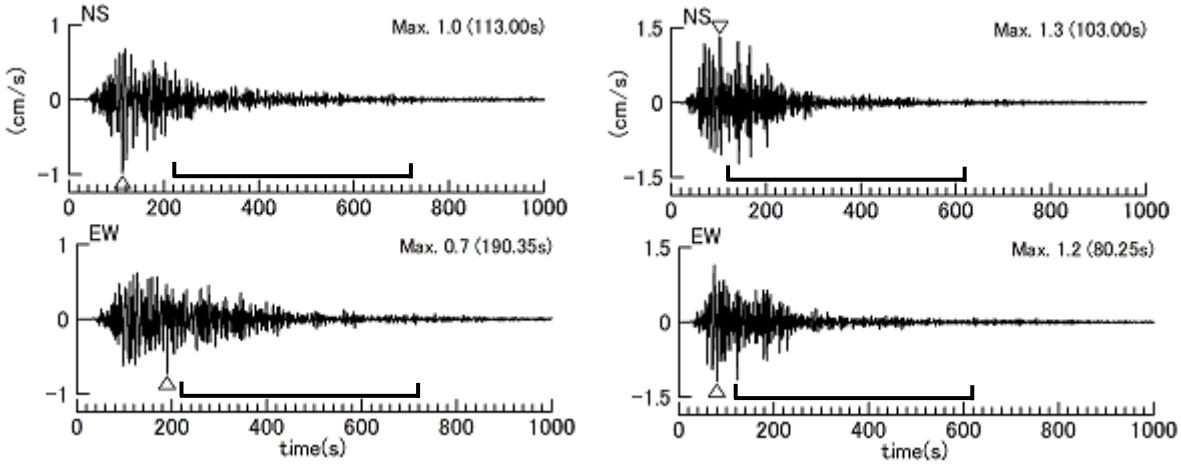

(a) YUKM (b) OYMM

Fig. 8 – Example of the observation waveforms（earthquake-No.6, 2014/11/22）

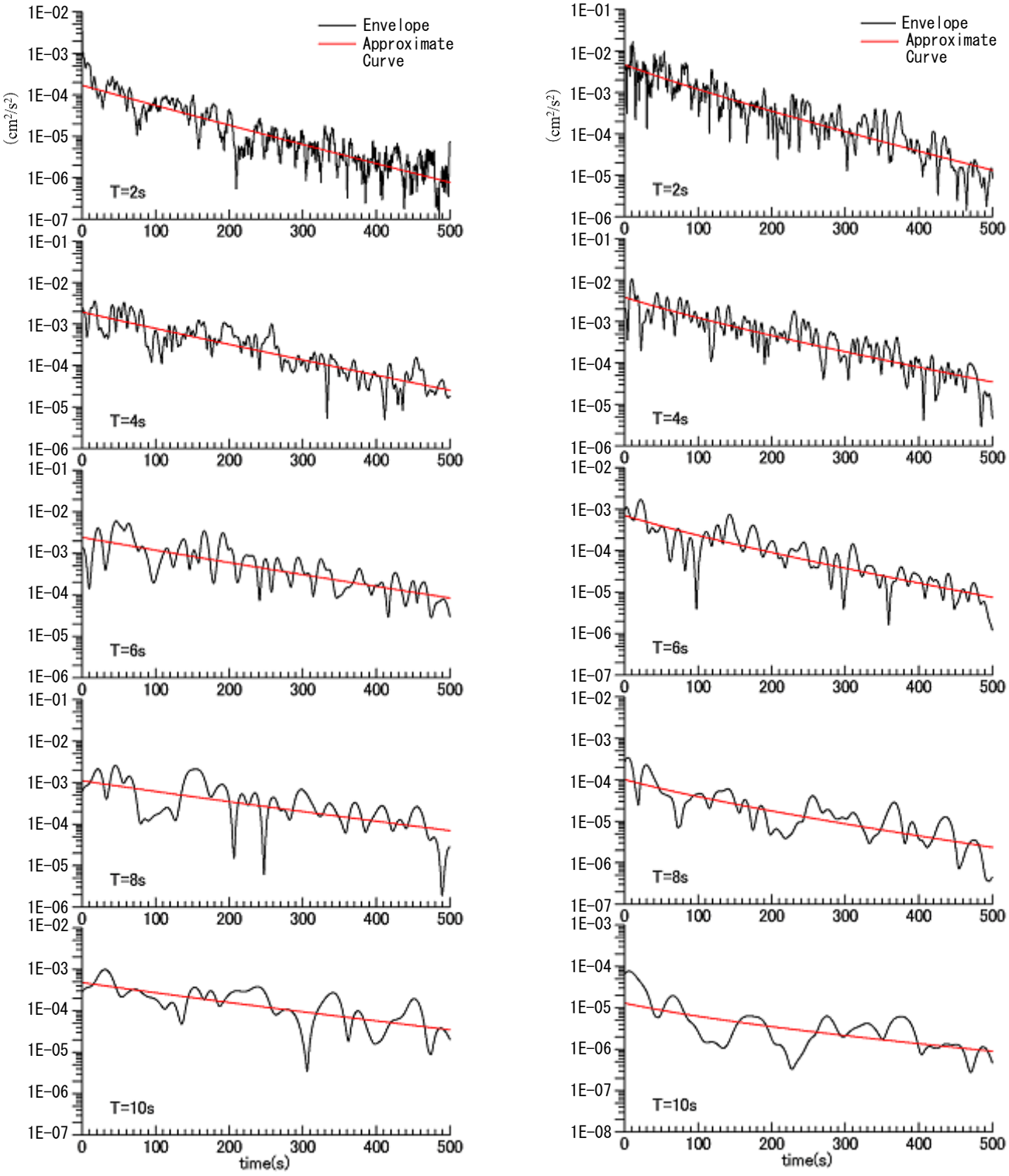

(a) YUKM

(b) OYMM

Fig. 9 – Comparison of the envelope waveforms and approximate curves in observation records

Figure 10 and Table 4 show the estimated Q values. The Q value exhibited a range of 160 to 380 at 0.1 to 0.5 Hz. The Q value is reduced below 0.11 Hz (more than 9 seconds), which corresponds to the vicinity of the predominant period in the Kanto basin. This suggests that the Q value may be affected by the transmission attenuation at the boundary of the mountain basin. By confirming the upper limit of the frequency at which the Q value decreases in this method, it may be possible to estimate the predominant period for the basin. Regardless of the structure immediately below the observation point, $Q = 490f^{0.41}$ was obtained as a regression equation above 0.125 Hz (period of 8 seconds or less) with a stable Q value gradient. The equation for the Q value used in the earthquake motion simulation was $Q = Q_0 f$. When this equation is used, the regression equation minimizing the error with $Q = 490f^{0.4}$ in the period of 2 to 4 seconds (the primary natural period of the high-rise and base-isolated structures) was observed to be $Q = 940f$.

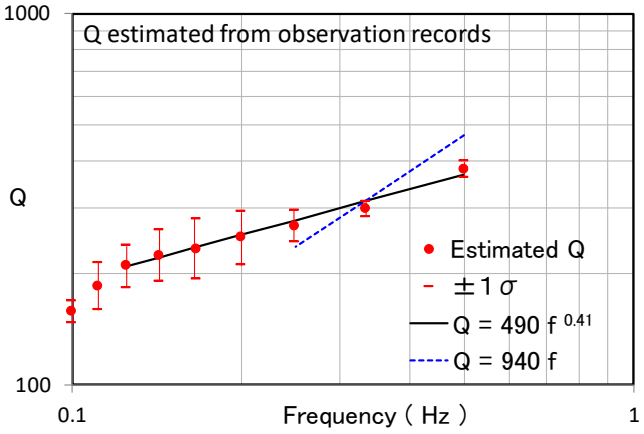

Fig. 10 – Q value and regression equation estimated from observation records

Table 4 – Q values estimated from observation records for the Kanto basin

(s)	(Hz)	Average .Q	1 σ
2	0.50	380	19.7
3	0.33	298	13.5
4	0.25	269	25.7
5	0.20	251	40.7
6	0.17	235	43.5
7	0.14	225	36.1
8	0.13	210	28.5
9	0.11	186	28.4
10	0.10	158	10.2

Underground structural models using $Q_0 = 940$ ($Q = 940\ f / fr$, $fr = 1.0$Hz) estimated by this study along with the conventional equation of $Q_0 = Vs / 5$ ($Q = Vs / 5 \cdot f / fr$, $fr = 0.5$Hz) in sedimentary layers were prepared. Earthquake motion simulations were also performed using these underground structural models. The earthquake and observation points used here were the same as those used for the Q value estimation. Figure 11 shows a comparison of the velocity waveforms (0.5 Hz low-pass filter processing, NS components) at each observation point. The arrow indicates the time when the maximum amplitude reaches 5% or less. The results for the $Q_0 = 940$ model show that the amplitude is up to 1.1 times greater, and the duration is up to 2.4 times greater than the amplitude of the $Q_0 = Vs / 5$ model. Furthermore, the envelope shapes of the seismic waveforms of both models of SRGM were observed to be different, and the difference in Q value affected the envelope shape.

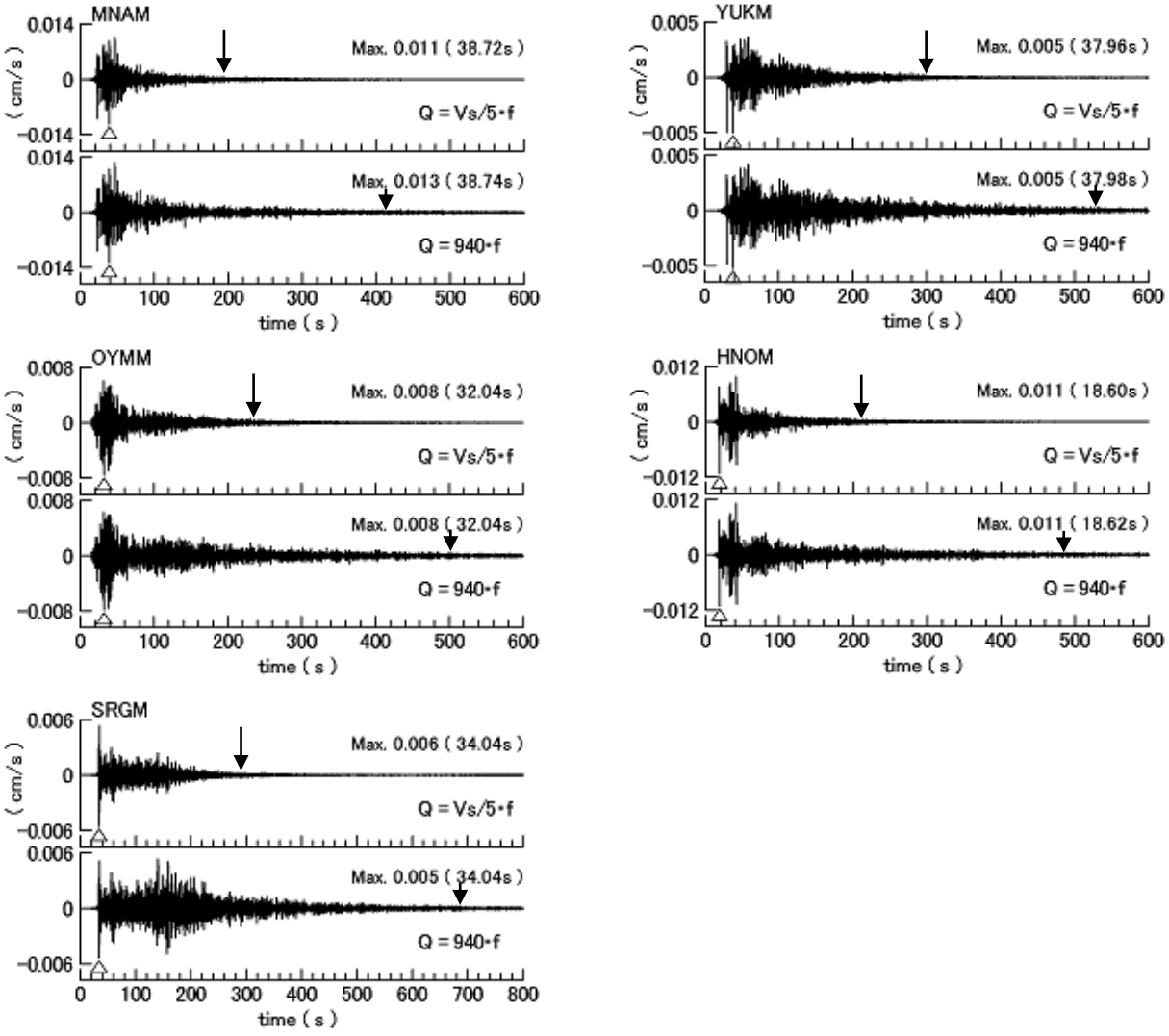

Fig. 11 – Simulation waveform(NS component) comparison
between Q_0 = Vs / 5 model and Q_0 = 940 model
（Note:arrows indicate the time when the maximum amplitude becomes 5% or less）

5. Conclusion

In our study, the applicability of the method for estimating attenuation characteristics of the sedimentary layer from the envelope of the subsequent waveform to the velocity waveform was first confirmed by a three-dimensional simulation. The Q values of the sedimentary layer were also estimated. As a result, we confirmed the frequency dependence of the Q value in the range of 0.1 to 0.5 Hz (2 to 10 seconds). For this range, the Q value was found to be between 160 to 380. Furthermore, the duration time of simulated waveforms using the estimated Q value was about twice as long as when the conventional Q value was used. By using long-lasting and long-period ground motions predicted by applying the Q value estimated in this study, it becomes possible to plan the structural design of high-rise or base-isolated buildings more appropriately. In the future, the applicability of this method to other basins will be examined. A three-dimensional simulation of a large earthquake in the Kanto basin using the Q value estimated by this method will also be performed.

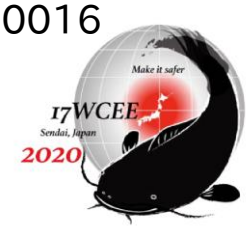

6. Acknowledgments

MeSO-net and GMS were used for this study.

7. References

[1] Kagawa T (2006): Attenuation Characteristics of Later Phases in Osaka Plain. *12th Japan Earthquake Engineering Symposium*, 1546-1549.

[2] Yoshida H, Sato Y, Kobayashi K, Sakai S, Hirata S (2016): Estimation of Q value of the Kanto Basin by using Earthquake Records of MeSO-net. *Summaries of Technical Papers of Annual Meeting Architectural Institute of Japan 2016.* B-2, 1069-1070.

[3] Sakai S, Hirata N (2009): Distribution of the Metropolitan Seismic Observation network. *Bulletin of the Earthquake Research Institute, University of Tokyo,* 84(2), 57-69.

[4] Dziewonski A, Bloch S, Landisman M (1969): A Technique for The Analysis of Transient Seismic Signals. *BSSA*, Vol.59, No.1, 427-444.

[5] Koketsu K, Miyake H, Fujiwara H, Hashimoto T (2008): Progress towards a Japan integrated velocity structure model and long-period ground motion hazard map. *Proc. 14WCEE,* Paper No.S10-038.

[6] Aoi S, Fujiwara H (1999): 3-D Finite-Difference Method Using Discontinuous Grids. *BSSA*, 89, 918-930.